Metabolomic Profiling of Aqueous Humor From Glaucoma Patients Identifies Metabolites With Anti-Inflammatory and Neuroprotective Potential in Mice

Monu Monu,[1] Bhoj Kumar,[2] Rahmat Asfiya,[3] Nariman Nassiri,[4] Vaama Patel,[5] Shibandri Das,[6] Sarah Syeda,[6] Mamta Kanwar,[6] Vivian Rajeswaren,[6] Bret A. Hughes,[6] Mark S. Juzych,[6] Akhil Srivastava,[3] Ashok Kumar,[6,7] and Pawan Kumar Singh[1]

[1]Department of Ophthalmology, Mason Eye Institute, University of Missouri School of Medicine, Columbia, Missouri, United States
[2]Complex Carbohydrate Research Center, University of Georgia, Athens, Georgia, United States
[3]Department of Pathology and Anatomical Sciences, University of Missouri School of Medicine, Columbia, Missouri, United States
[4]Glaucoma Division, Department of Ophthalmology, UCLA Doheny Eye Institute, Pasadena, California, United States
[5]Department of Ophthalmology, Vanderbilt Eye Institute, Nashville, Tennessee, United States
[6]Department of Ophthalmology, Visual and Anatomical Sciences, Kresge Eye Institute, Wayne State University School of Medicine, Detroit, Michigan, United States
[7]Department of Biochemistry, Microbiology, and Immunology, Wayne State University School of Medicine, Detroit, Michigan, United States

Correspondence: Pawan Kumar Singh, Department of Ophthalmology, Mason Eye Institute, University of Missouri School of Medicine, 1 Hospital Drive, Columbia, MO 65212, USA; pksfcq@health.missouri.edu.
Ashok Kumar, Department of Ophthalmology, Visual and Anatomical Sciences, Kresge Eye Institute, 4717 Saint Antoine, K-416, Detroit, MI 48084, USA; akuma@med.wayne.edu.

Received: March 3, 2025
Accepted: April 13, 2025
Published: May 22, 2025

Citation: Monu M, Kumar B, Asfiya R, et al. Metabolomic profiling of aqueous humor from glaucoma patients identifies metabolites with anti-inflammatory and neuroprotective potential in mice. *Invest Ophthalmol Vis Sci.* 2025;66(5):28. https://doi.org/10.1167/iovs.66.5.28

Purpose. Metabolomic profiling of aqueous humor from primary open-angle glaucoma (POAG) patients using targeted metabolomics analysis and assessment of the potential anti-neuroinflammatory and neuroprotective roles of key dysregulated metabolites in a mouse model of retinal neuroinflammation.

Methods. A targeted metabolomics was performed on aqueous humor from POAG patients ($n = 19$) and healthy subjects ($n = 10$) via LC-MS/MS. In vitro neuroprotection studies were performed using a mouse cone photoreceptor cell line (661W) exposed to oxidative stress. For in vivo therapeutic studies, a few key dysregulated metabolites were delivered either topically via extracellular vesicle (EV)-mediated delivery or intravitreally into a C57BL/6 mouse model of retinal neuroinflammation. The neuroprotective and anti-neuroinflammatory properties were determined in the presence and absence of metabolites through pattern electroretinography, TUNEL, and quantitative PCR analyses.

Results. Among the 135 endogenous metabolites identified, 31 metabolites showed significant dysregulation in POAG. Metabolite set enrichment analysis revealed that these altered metabolites were associated with dysregulation of multiple key cellular pathways, including glycolysis, pentose phosphate pathway, short-/long-chain fatty acid metabolism, mitochondrial β-oxidation, and electron transport chain under glaucomatous conditions. Among these differentially expressed metabolites, a putative neuromodulator (agmatine) and a vitamin (thiamine) significantly decreased in POAG patients. Intravitreal or EV-mediated topical delivery of agmatine and thiamine significantly reduced the inflammatory response and protected retinal ganglion cell function against neuroinflammatory damage in the mouse retina. Agmatine and thiamine treatment also significantly protected photoreceptor cells from oxidative stress–induced cell death and attenuated the inflammatory cytokine response.

Conclusions. Our results revealed significant metabolic alterations in POAG that affect key cellular functions. Agmatine and thiamine could be potential immunomodulatory or neuroprotective drugs to treat or prevent neuroinflammatory damage to the retina during glaucoma.

Keywords: metabolomics, glaucoma, neuroinflammation, neuroprotection, agmatine, thiamine, EVs, drug delivery

Glaucoma is a progressive optic neuropathy characterized by the gradual degeneration of retinal ganglion cells (RGCs) and their axons.[1,2] It is one of the leading causes of irreversible blindness worldwide in individuals 40 to 80 years old. Glaucoma currently affects approximately 90 million people, and, due to the aging population, it is

Investigative Ophthalmology & Visual Science

estimated to surpass 112 million people by 2040.[1,3] The etiology of this multifactorial disease is poorly understood. Although various risk factors, including genetic predispositions, environmental factors, and physiological conditions, influence the onset of glaucoma, elevated intraocular pressure (IOP) is the primary and only modifiable risk factor known for this disease. Controlling IOP slows the progression of the disease, but currently there is no cure for glaucoma. In addition to IOP elevation, various other pathological mechanisms, such as immune system dysregulation, neuroinflammation, alterations in neurotrophin signaling, mitochondrial dysfunction, protein misfolding (endoplasmic reticulum stress), oxidative stress, metabolic abnormalities, and vascular dysfunction, have been proposed to contribute to glaucomatous neurodegeneration.[2,4,5] Among these pathogenic mechanisms, neuroinflammation is one of the key players in RGC death and loss[2,4]; however, no neuroprotective therapies are currently available to prevent RGC damage in glaucoma. Thus, identifying novel neuroprotective targets is crucial for preventing or treating visual impairment in glaucoma patients.

Over the past decade, the multiomics approaches, including genomics, proteomics, lipidomics, and metabolomics studies in glaucoma, have not only helped researchers provide complementary insight into the pathologic mechanisms of this disease but also provided an ideal tool for detecting biomarkers and therapeutic targets.[6,7] Metabolomics is the study of profiling metabolites in cells, tissues, or biofluids, and it has served as a key tool for biomarkers and therapeutic discoveries in several diseases, including ocular diseases.[8] Metabolites are essential components of cellular and physiological processes that help maintain tissue health and repair mechanisms and establish cellular homeostasis.[9,10] Several metabolites play crucial roles in maintaining ocular health, including maintaining nutrient supply,[11] regulating cellular functions,[12] and integrity,[13] protecting against oxidative stress[14] and inflammation,[15] supporting energy production, and influencing the neurological functions of the retina.[16] Recent metabolomics studies from glaucoma subjects using blood plasma and aqueous humor have demonstrated metabolic alterations in glaucoma.[17,18] Similarly, a few metabolomics studies showing metabolic changes in aqueous humor have been performed using experimental models of glaucoma.[19] These studies have revealed alterations in multiple metabolites that are involved in steroid biosynthesis, senescence, biotin and beta-alanine metabolism, taurine and spermine metabolism, glutamine and glutamate metabolism, and trace amine-associated receptor 1.[6,17,20–23] All of these independent studies provide insights into metabolic dysregulations and reveal a new set of metabolites altered in glaucomatous conditions. Despite multiple studies exploring metabolomic changes in various tissue matrices, out of >150,960 known human metabolites (listed on https://hmdb.ca/), only a partial metabolome analysis with some specific metabolites can be identified with one method at a given time.[24] Moreover, because many isomeric metabolites are present, multiple metabolomics studies of glaucomateous aqueous humor are needed.[6] Thus, further profiling of metabolomic changes in glaucoma is essential to establish a comprehensive list of altered metabolites that could serve as biomarkers for early detection or therapeutic targets to treat or prevent vision loss in glaucoma patients.

In the present study, we aimed to perform a targeted metabolomics study to identify the levels of differentially expressed metabolites in the aqueous humor of primary open-angle glaucoma (POAG) patients and test the anti-neuroinflammatory and neuroprotective potential of some of the key metabolites in a preclinical model of retinal neuroinflammation. Here, we report significant dysregulation of 31 metabolites in glaucoma patients compared with healthy controls. Moreover, we demonstrated the anti-inflammatory and neuroprotective roles of a putative neuromodulator and a polyamine family metabolite, agmatine, and a vitamin, thiamine, whose levels were significantly reduced in glaucoma patients.

Materials and Methods

Patient Population and Aqueous Humor Collection

This was a prospective study conducted in accordance with the tenets of the Declaration of Helsinki. All patients were candidates for either cataract or glaucoma surgery and signed a preoperative informed consent form with approval to use their extracted aqueous humor for research. The study design and protocol were approved by the Wayne State University (WSU) Institutional Review Board (IRB #104517M1X). The exclusion criteria included patients younger than 18 years; a history of any inflammatory ocular diseases (such as uveitis or endophthalmitis), diabetic retinopathy, closed-angle glaucoma, or secondary glaucoma; any intraocular surgery within a year in the study eyes; or current or recent topical steroid use. Undiluted aqueous humor (~100 µL) was collected via anterior chamber paracentesis at the beginning of surgery. A total of 29 patients (POAG, $n = 19$; healthy, $n = 10$) participated in this study. The samples were immediately snap-frozen in liquid nitrogen and transferred to a −80°C freezer for storage and analysis.

Targeted Metabolomics Analysis

Liquid Chromatography-Tandem Mass Spectrometry Analysis. To cover a broad range of metabolites, targeted metabolomics analysis was performed at the Pharmacology and Metabolomics Core, Karmanos Cancer Institute, Wayne State University, using a method reported previously.[25] This targeted metabolomics platform consists of three different chromatographic separation methods, including reversed-phase liquid chromatography (RP-LC), hydrophilic interaction liquid chromatography (HILIC), and ion-pair liquid chromatography (IP-LC). It was developed to quantitatively determine ~250 endogenous metabolites with diverse physicochemical properties that are involved in major metabolic pathways, including glycolysis, pentose phosphate pathway, tricyclic acid cycle, nucleotide and nucleoside metabolism, amino acid metabolism, and fatty acid metabolism. Briefly, an equal volume (~100 µL) of aqueous humor was transferred into a new 2-mL centrifuge tube, and samples were extracted with a 4× volume of ice-cold methanol and again with 100 µL of 80% methanol. The supernatants from both rounds of extraction were combined and dried using a cold trap concentrator. The dried samples were first reconstituted in 150 µL of 50% acetonitrile (ACN) and further diluted in ACN for HILIC and in H_2O for RP-LC and IP-LC. All liquid chromatography-tandem mass spectrometry (LC-MS/MS) analysis was performed using an QTRAP 6500 system (SCIEX, Framingham, MA, USA)

coupled with a Nexera ultra-high-performance liquid chromatography (UHPLC) system (SHIMADZU, Kyoto, Japan)

Chromatographic separation of small organic acids, amino acid metabolites, nucleobases, nucleosides, monophosphate nucleosides, sugar derivatives, and fatty acid derivatives was achieved based on RP-LC on a Synergi Polar-RP column (80 Å, 2.0 mm × 150 mm, 4 µm; Phenomenex, Torrance, CA, USA) via a gradient of mobile phase A (0.03% formic acid) and mobile phase B (0.03% formic acid in ACN) at a flow rate of 0.25 mL/min and a column temperature of 40°C. The separation of highly polar metabolites with poor retention or dynamic ranges on RP-LC was achieved using an Atlantis HILIC silica column (2.1 mm × 150 mm, 3 µm; Waters Corporation, Milford, MA, USA) with a gradient of mobile phase A (10-mM ammonium formate, pH 3.0) and mobile phase B (0.1% formic acid in ACN) at a flow rate of 0.25 mL/min and a column temperature of 40°C. Metabolites such as coenzyme A and its derivatives; mono-, di-, or triphosphate nucleotides; and sugar phosphates were detected via the IP-LC mechanism with an Atlantis T3 column (2.1 mm × 100 mm, 3.0 µm; Waters Corporation). The gradient elution consisted of mobile phase A (100-mM hexofluoro-2-propanol and 8.6-mM triethylamine in water, final pH 8.3) and mobile phase B (10% ACN in mobile phase A) at a flow rate of 0.5 mL/min and a column temperature of 40°C. The data were analyzed in both positive and negative ionization modes via multiple reaction monitoring. The detailed chromatographic gradient conditions and mass spectrometric parameters were described previously.[25] Metabolite reference standards for each metabolite and quality control (QC) samples were prepared and utilized for the analysis as described previously.[25]

Data Acquisition and Processing. The LC-MS/MS data were acquired using Analyst 1.6 and processed and quantified using MultiQunat 3.0 software. The raw data were converted to mzData format using Mass Hunter Qualitative Analysis Software (Agilent, Santa Clara, CA, USA) and then imported into the R package xcms (R Foundation for Statistical Computing, Vienna, Austria) for preprocessing. The default parameters of the xcms software were used. The preprocessed data were obtained using three features of the dataset: retention time, mass-to-charge ratio (m/z), and peak intensity. The annotation was performed via the R package CAMERA to annotate isotope peaks, adducts, and fragments.[26] The data were normalized for each sample and used for statistical analysis.

Postprocessing and Data Analysis. Both univariate and multivariate analyses of the metabolomics data were performed using MetaboAnalyst 6.0 (https://www.metaboanalyst.ca). A default data integrity check was performed on the raw data, and missing values were imputed with the median value within the group. The data were median normalized and $\log_{10}$ transformed. The relationships between datasets were assessed using Spearman correlation analysis. Multivariate discrimination between cases and controls was performed via principal component analysis (PCA) and partial least squares discriminant analysis (PLS-DA). Hierarchical clustering of samples and metabolites was conducted using Euclidean distance and the Ward's linkage algorithm (Ward.D). The important metabolites and sample outliers were identified using a random forest classification method. Univariate analysis was performed via Student's t-test. The $\log_2$ fold change (FC) was calculated, and metabolites with FC $\geq$ 2 and $P \leq 0.05$ were considered statistically significant. These criteria were visualized using a volcano plot, with an FC cutoff of 2 on the x-axis and a P value threshold of 0.05 on the y-axis. Pathway analysis was performed using metabolite set enrichment analysis (MSEA) and the Kyoto Encyclopedia of Genes and Genomes (KEGG) metabolic pathway database.

Cell Culture and Treatment

For the neuroprotection study, the neuronal mouse cone photoreceptor cell line 661W was used as described in our previous studies.[27,28] The 661W cells were provided by Muayyad Al-Ubaidi, PhD (Department of Cell Biology, University of Oklahoma Health Sciences Center, Oklahoma City, OK, USA).[29] The 661W cell line was cultured and maintained in Dulbecco's Modified Eagle Medium (DMEM) supplemented with 10% fetal bovine serum (FBS), 10-µg/mL L-glutamine, 1× penicillin–streptomycin, 40-µg/L hydrocortisone, 40-µg/L progesterone, 32-mg/L putrescine, and 40-µL/L β-mercaptoethanol. Photoreceptor cell death was induced by challenging 661W cells with H_2O_2 (100 µM) for 24 hours in the presence or absence of agmatine or thiamine (100 ng/mL). Oxidative stress-induced cell death and neuroprotection by these metabolite treatments were assessed via TUNEL staining using an ApopTag Fluorescein In Situ Apoptosis Detection Kit (Sigma-Aldrich, St. Louis, MO, USA) per the manufacturer's instructions. The TUNEL-stained slides were visualized using a Keyence microscope (Keyence, Itasca, IL, USA).

For neuroinflammation studies, photoreceptor cells were stimulated with Toll-like receptor 2 (TLR2; Pam3, 100 ng/mL), TLR3 (polyinosinic–polycytidylic acid [poly I:C], 100 ng/mL), and TLR4 (lipopolysaccharide [LPS], 100 ng/mL) agonists in the presence or absence of agmatine or thiamine for 24 hours. The treated and untreated cells were harvested in TRIzol (Invitrogen, ThermoFisher Scientific, Rockford, IL, USA), and the levels of pro-inflammatory mediators were measured via by quantitative PCR (qPCR).

Animals and Ethics Statement

C57BL/6 wild-type (WT) mice were purchased from The Jackson Laboratory (Bar Harbor, ME, USA) and maintained at the WSU or the University of Missouri (MU) School of Medicine Office of Animal Resources (OAR) facility. Both male and female mice 6 to 10 weeks of age were used for all of the experiments. All animals were housed in a controlled-access Association for Assessment and Accreditation of Laboratory Animal Care (AAALAC)-approved OAR facility, maintained under a 12-hour light/dark cycle, and fed a lab diet rodent chow (PicoLab; LabDiet, St. Louis, MO, USA) and water ad libitum. The mice were treated in compliance with the ARVO Statement for the Use of Animals in Ophthalmic and Vision Research. All biohazard and animal procedures were approved by the Institutional Biosafety Committee and the Animal Care and Use Committee of the WSU and MU.

Induction of Retinal Inflammation

To assess the neuroprotective role of agmatine and thiamine in vivo, retinal inflammation was induced by intravitreal injection of TLR agonists: TLR2 (Pam3, 0.1 µg/eye), TLR3 (poly I:C, 0.1 µg/eye), or TLR4 (LPS, 0.1 µg/eye). Six hours after the TLR agonist injection, the mice were treated either with a single intravitreal injection of agmatine or thiamine

Investigative Ophthalmology & Visual Science

(0.1 µg/eye) or once a day via eye drops using EVs loaded with agmatine (0.1 µg/eye drop). At 48 hours post-treatment, pattern electroretinography (pERG) was performed to assess the RGC function. Following euthanasia, the neuronal retina was harvested in TRIzol to assess the levels of inflammatory cytokines via qPCR.

EV Purification and Drug Loading

EV Isolation and Characterization. EVs were isolated from normal human primary trabecular meshwork cells (HTMCs) using the classical high-speed ultracentrifugation method with slight modifications.[30,31] Briefly, HTMCs were cultured in DMEM supplemented with 10% (v/v) heat-inactivated exosome-free FBS (System Biosciences, Palo Alto, CA, USA) and 1× penicillin–streptomycin solution. Upon reaching 80% to 90% confluency, the culture supernatant was collected and centrifuged at 2000*g* for 5 minutes to remove cell debris, followed by centrifugation at 10,000*g* for 30 minutes to remove large vesicles (microvesicles). The clear supernatant was then filtered through a 0.2-µm syringe filter, followed by ultracentrifugation at 110,000*g* for 120 minutes at 4°C using a 70.2 Ti rotor (Optima XPN-80; Beckman Coulter, Brea, CA, USA) to pellet the EVs. The EV pellet was carefully separated from the supernatant and resuspended in 1× PBS. The EVs were characterized per the minimal information for studies of extracellular vesicles (MISEV2023) guidelines.[32] EV size and morphology were assessed via transmission electron microscopy (TEM). The number and size of the purified EVs were estimated using Nanoparticle Tracking Analysis (NTA; NanoSight NS300; Malvern Panalytical, Malvern, *UK*). Immunoblotting was performed using the EV-specific marker CD63 to ensure the purity of the isolated EVs.

Synthesis and Characterization of the EV–Agmatine Complex. Agmatine was loaded into HTMC-purified EVs using a heat and cold shock method[33] modified in Srivastava's laboratory. Briefly, 2 mg of EVs (based on total protein estimation) and 2 mg of agmatine were thoroughly mixed in 2 mL of 1× PBS with slight agitation at 37°C. The mixture was then incubated at 42°C for 1 minute, followed by incubation on ice for 5 minutes. The heat/cold shock procedure was repeated three times. The EV–agmatine mixture was then briefly sonicated for 15 seconds and incubated on ice for 2 minutes. This procedure was also repeated three times, after which the EV–agmatine mixture was incubated at 37°C for 2 hours with shaking at 120 rotations per minute. Finally, the EV–agmatine complex was diluted with 1× PBS to 5 mL and concentrated to 500 µL volume using an Amicon 10-kDa molecular weight cutoff membrane filter (Sigma-Aldrich, St. Louis, MO, USA) to purify the complex and remove unbound agmatine. Following purification, qualitative and quantitative characterization of the EV–agmatine complexes was performed via LC-MS/MS, TEM, and NTA.

RNA Extraction and Quantitative RT-PCR

Total RNA was extracted from in vivo and in vitro tissue/cell samples using TRIzol per the manufacturer's instructions. cDNA was synthesized from 1 µg of total RNA using a Maxima First Strand cDNA Synthesis Kit for RT-qPCR (ThermoFisher Scientific) per the manufacturer's instructions. The cDNA was amplified using gene-specific PCR primers using the QuantStudio 3 Real-Time PCR System (ThermoFisher Scientific). The relative expression of inflammatory cytokine genes was normalized in proportion to the constitutive gene β-actin as an internal control and quantitatively analyzed using the $\Delta\Delta C_T$ method, represented as FC expression.

Data Availability

The metabolomics metadata are available on: https://github.com/bhojkumar-phd/Metabolomic-POAG.git.

Pattern Electroretinography

pERG was used to determine RGC function and neuroprotection in the treated and untreated groups using the Celeris pERG system (Diagnosys, Lowell, MA) per the manufacturer's recommendations. Briefly, dark-adapted mice were anesthetized with a ketamine (75 mg/kg) and xylazine (10 mg/kg) solution. Eyes were dilated and numbed using 1% tropicamide and 0.5% proparacaine ophthalmic drops, respectively. The mouse was placed on the Diagnosys Celeris platform, heated to 37°C), and GenTeal lubricant eye gel (Alcon, Fort Worth, TX, USA) was applied before recording to prevent dryness and to establish contact between the stimulators and the eye. pERG was recorded using the Diagnosys Celeris pERG stimulator, which generates visual stimulus by black and white, alternating contrast, reversing bars with a spatial frequency of 0.125 cyc/deg, a luminescence of 50 cd/m^2, and contrast of 100%. The flash stimulator was used as a reference electrode on the contralateral eye. Each pERG was an average of 600 sweeps at an interval of 1 second. The first positive peak was designated as P1, and the second negative peak was designated as N2. The amplitude was measured from P1 to N2. The means of the P1–N2 amplitudes (presented as pERG wave amplitude) in eyes injected with Pam3, LPS, or poly I:C were compared to control, and agmatine- and thiamine-treated eyes were compared to the Pam3-, LPS-, and poly I:C–challenged eyes. The data were analyzed using Diagnosys Espion 6 software and presented as the average wave amplitude from both eyes.

Statistical Analysis

The statistical differences between the experimental groups were analyzed using Prism 10.1.2 (GraphPad Software, Boston, MA, USA). One-way analysis of variance (ANOVA) and two-way ANOVA were used to compare the significance levels between experimental groups, as indicated in the figure legends. A value of $P < 0.05$ was considered statistically significant. All data are expressed as mean ± standard deviation (SD) from three biological replicates unless indicated otherwise.

Results

Patient Demographics

All patients enrolled in this study were candidates for cataract or glaucoma surgery. A total of 29 aqueous humor samples were collected from 29 different patients (29 eyes). Among these, 19 were POAG patients, and 10 were healthy controls. The mean age of all patients was 70.8 years (range, 53–84); 12 subjects were male, and 17 were female. The demographics, comorbid clinical conditions, and medica-

Table 1. Demographic Data, Ophthalmologic Features, Glaucoma Medications, and Comorbid Clinical Conditions of Individuals With POAG Compared With Controls

	POAG (n = 19)	Controls (n = 10)
Age (y), mean ± SD	69.6 ± 7.5	73.1 ± 8.6
Males, %	47.4	30
Females, %	52.6	70
IOP (mmHg), mean ± SD	17.19 ± 6.7	14.94 ± 2.2
Visual acuity (logMAR), mean ± SD	0.60 ± 0.6	0.37 ± 0.4
Central corneal thickness (µm), mean ± SD	518.7 ± 25.2	563.6 ± 43.1
Retinal nerve fiber layer thickness (µm), mean ± SD	63.15 ± 18.7	82.5 ± 6.2
Visual field mean deviation (dB)	−10.07	—
Glaucoma severity, %		
Mild	35	—
Moderate	20	—
Severe	45	—
Glaucoma medications, %		
Prostaglandins	55	—
Carbonic anhydrase inhibitors	50	—
β-Blockers	25	—
α-Adrenergic agonists	35	—
Rho kinase inhibitor	5	—
Nitric oxides	5	—
Diabetes (without diabetic retinopathy), %	15	10
Other systemic diseases, %		
Hypertension	45	50
Hypercholesterolemia	30	30
Thyroid disease	15	10

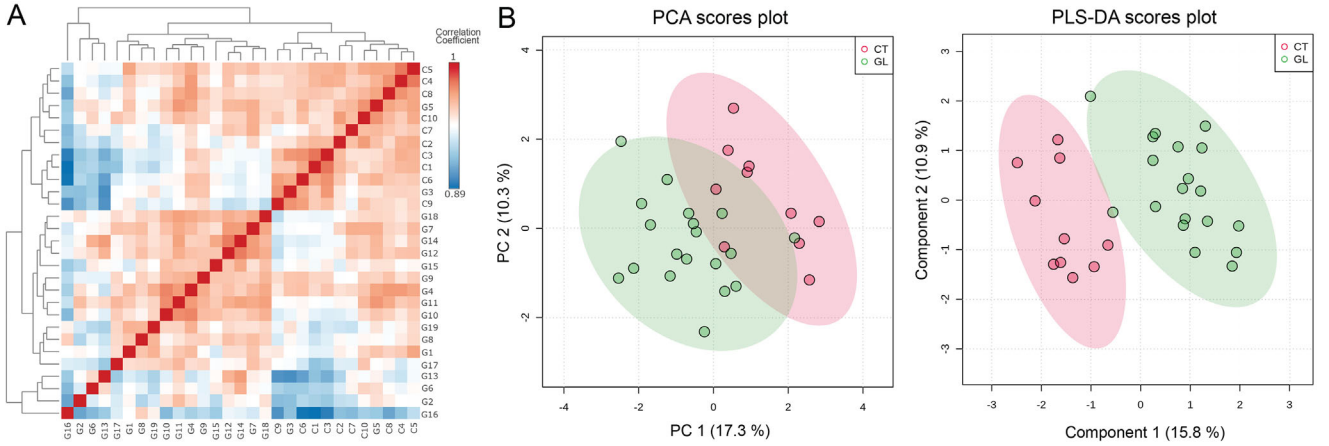

Figure 1. Metabolic profiling of aqueous humor distinguishes healthy controls from patients with POAG. (**A**) Spearman's correlation heatmap of pairwise sample comparisons within the aqueous humor metabolomes of healthy controls (n = 10, C1–C10) and POAG patients (n = 19, G1–G19). The color gradient reflects the strength and direction of the correlations. (**B**) PCA and PLS-DA plots demonstrate the separation of the control (CT) and POAG (GL) groups on the basis of their distinct metabolic profiles.

tions used by the enrolled patients are summarized in Table 1.

Metabolomic Alterations in the Aqueous Humor of POAG Patients

To investigate the metabolic alterations in POAG, we performed targeted metabolomics analyses of aqueous humor samples from healthy controls and POAG patients. Three distinct chromatographic separation methods (RP-LC, HILIC, and IP-LC) were employed, coupled with positive and negative mode mass spectrometry. Among the 241 database-matched metabolites, 135 that were consistently detected in all of the subjects were selected for quantitative analysis using MetaboAnalyst. These 135 metabolites that were uniformly present in all subjects were further used for multivariate analysis such as PCA and discriminant analysis (PLS-DA), as well as for clustering analysis.

Spearman correlation analysis with hierarchical clustering revealed three primary sample clusters. The POAG patient samples predominantly clustered together, with the exceptions of subjects G3 and G5, suggesting substantial metabolic changes associated with glaucoma. The lower Spearman correlation coefficients within the POAG group than in the control group indicate greater interindividual metabolic variability in glaucoma patients (Fig. 1A). PCA revealed partial separation of the control and POAG groups, reflecting inherent biological variation within the

Investigative Ophthalmology & Visual Science

Table 2. Top 30 DEMs Showing Significant Alterations in POAG Patients

Row	Compound	*t*	*P*	FC	Log_2FC	$-Log_{10}$ (*P*)	FDR
1	L-Aspartic acid	6.799	6.06E-07	0.24	−2.05	6.217	8.18E-05
2	Agmatine	6.922	2.23E-06	0.14	−2.86	5.652	0.000
3	Putrescine	6.629	3.47E-06	0.14	−2.88	5.460	0.000
4	Nicotinic acid mononucleotide	4.488	0.000	0.28	−1.84	3.907	0.004
5	Thiamine	4.308	0.000	0.28	−1.84	3.707	0.005
6	Thymidine	−3.481	0.002	1.65	0.72	2.685	0.046
7	Creatinine	−3.348	0.004	1.32	0.40	2.436	0.071
8	*N*-Acetylputrescine	−3.093	0.006	1.65	0.72	2.234	0.098
9	Flavone	2.878	0.010	0.60	−0.74	1.992	0.148
10	C8 carnitine (octanoyl-L-carnitine)	−3.048	0.011	6.46	2.69	1.960	0.148
11	Hydroxyisocaproic acid	−2.670	0.014	2.19	1.13	1.869	0.166
12	Indole	−2.483	0.020	2.15	1.10	1.709	0.197
13	*cis*-Aconitic acid same as M007	−2.622	0.020	1.72	0.78	1.703	0.197
14	*N*-Alpha-acetyllysine	−2.503	0.020	1.36	0.45	1.690	0.197
15	C5:0 carnitine (valeryl-L-carnitine)	−2.418	0.030	1.66	0.73	1.525	0.269
16	Aminoadipic acid	−2.138	0.042	1.41	0.49	1.374	0.318
17	2-Ketohexanoic acid_neg	−2.158	0.042	1.31	0.39	1.372	0.318
18	AICA-riboside	−2.154	0.044	1.82	0.87	1.353	0.318
19	*N*-Acetylglutamine	−2.117	0.045	1.36	0.45	1.343	0.318
20	Dimethylamine	−2.216	0.050	1.29	0.37	1.305	0.318
21	Xanthosine	−2.078	0.050	8.37	3.07	1.303	0.318
22	L-Proline	−2.070	0.052	1.33	0.41	1.286	0.318
23	*S*-Adenosylhomocysteine	−1.998	0.064	1.50	0.59	1.196	0.358
24	1-Methylhistidine	−1.987	0.066	1.30	0.38	1.183	0.358
25	Cyclic AMP	−1.893	0.070	1.20	0.27	1.153	0.358
26	Choline	−1.894	0.071	1.25	0.33	1.148	0.358
27	Guanidinoacetic acid	−1.909	0.075	1.43	0.51	1.124	0.358
28	Hypoxanthine	−1.851	0.076	1.99	0.99	1.121	0.358
29	Dihydroxyacetone phosphate + M097	1.903	0.077	0.66	−0.60	1.114	0.358
30	2-Aminobenzoic acid	−1.833	0.081	1.71	0.77	1.091	0.365
31	L-Homocysteine	−1.743	0.097	1.87	0.90	1.014	0.419

POAG samples. PCA revealed 17.3% and 10.3% of the variance in principal component 1 (PC1) and PC2, respectively (Fig. 1B). To enhance group separation and identify discriminatory metabolites, we performed supervised PLS-DA, which further distinguished the two groups, showing 15.8% and 10.9% of the variance in PC1 and PC2, respectively (Fig. 1B).

By performing a quantitative analysis of 135 endogenous metabolites in the aqueous humor, we identified 31 differentially expressed metabolites (DEMs) that were significantly altered in POAG patients compared with control subjects (Table 2). These metabolites belong to the carbohydrate (dihydroxyacetone phosphate), lipid (choline), DNA (xanthosine, hypoxanthine, thymidine), amino acid (aspartic acid, proline), vitamin (thiamine, nicotinic acid mononucleotide), and polyamine (carnitine, putrescine, agmatine) families and showed dysregulation in the aqueous humor of POAG patients compared with healthy subjects. These DEMs were further subjected to hierarchical clustering analysis using Euclidean distance and Ward's linkage algorithms, which revealed distinct expression patterns of the top 25 DEMs (Fig. 2A). To further validate the discriminatory power of these altered metabolites, we performed random forest classification analysis, which identified the top 15 metabolites based on their mean decrease accuracy (Fig. 2B).

The volcano plot analysis revealed 31 significant DEMs (24 upregulated and seven downregulated) (Fig. 3A; Table 2). Among these, agmatine, L-aspartic acid, nicotinic acid mononucleotide, putrescine, and thiamine were significantly decreased in POAG patients, whereas octanoyl-L-carnitine, hydroxyisocaproic acid, hypoxanthine, indole, and xanthosine were elevated. Box-and-whisker plots were used to depict the expression profiles of these key altered metabolites in POAG patients with respect to controls (Fig. 3B).

MSEA of the DEMs revealed dysregulation of multiple key metabolic pathways, including the pentose phosphate pathway, ketone body metabolism, glycolysis, butyrate metabolism, mitochondrial beta-oxidation of long- and short-chain fatty acids, the Warburg effect, the mitochondrial electron transport chain, carbohydrate metabolism, DNA metabolism, and the metabolism of multiple amino acids (Fig. 4). Together, these findings demonstrate significant alterations in the aqueous humor metabolite profiles of POAG patients compared with those of healthy controls, affecting essential cellular metabolic pathways.

Agmatine and Thiamine Attenuated the Inflammatory Response and Protect Against Oxidative Stress–Induced Retinal Neuronal Death In Vitro

Among the top five downregulated metabolites, we discovered decreased levels of a putative neuromodulator and l-arginine metabolite agmatine and the vitamin thiamine in glaucoma patients. Therefore, first, we aimed to test the anti-neuroinflammatory and neuroprotective effects of these metabolites in vitro using the 661W neuronal photorecep-

Investigative Ophthalmology & Visual Science

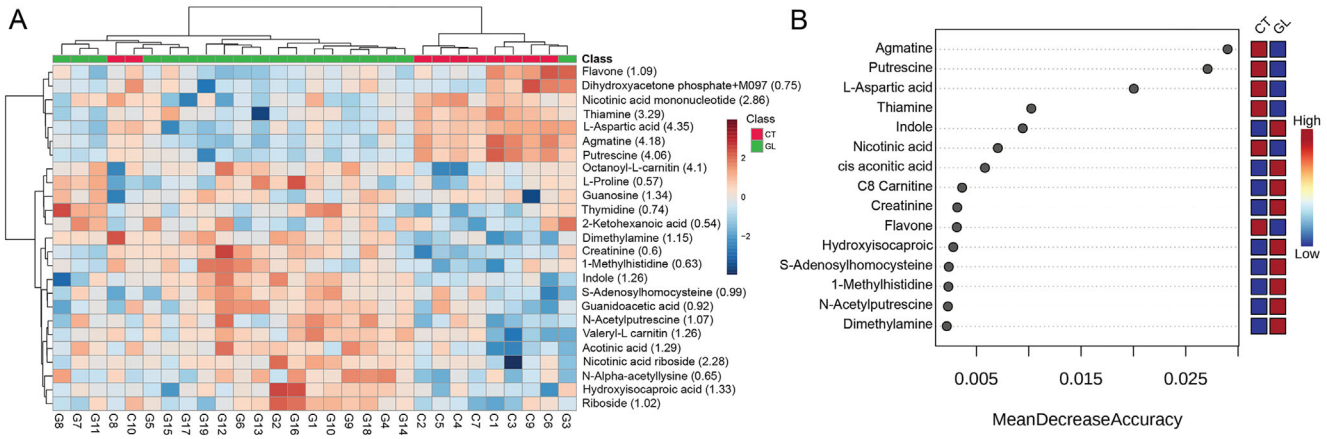

Figure 2. Hierarchical clustering and random forest analyses of metabolites. (**A**) Heatmap displaying hierarchical clustering of the top 25 metabolites, ranked by the variable importance in projection (VIP) score, in the control (CT, *red*) and POAG (GL, *green*) samples. Clustering was performed using Euclidean distance and Ward's linkage algorithm. The *x*-axis represents samples, and the *y*-axis represents metabolites. The *red/blue* color gradient indicates metabolite levels across samples. The respective VIP scores are displayed in parentheses after the metabolite labels. (**B**) The random forest classification model emphasizes the significance of the top 15 DEMs, ranked according to their impact on classification accuracy.

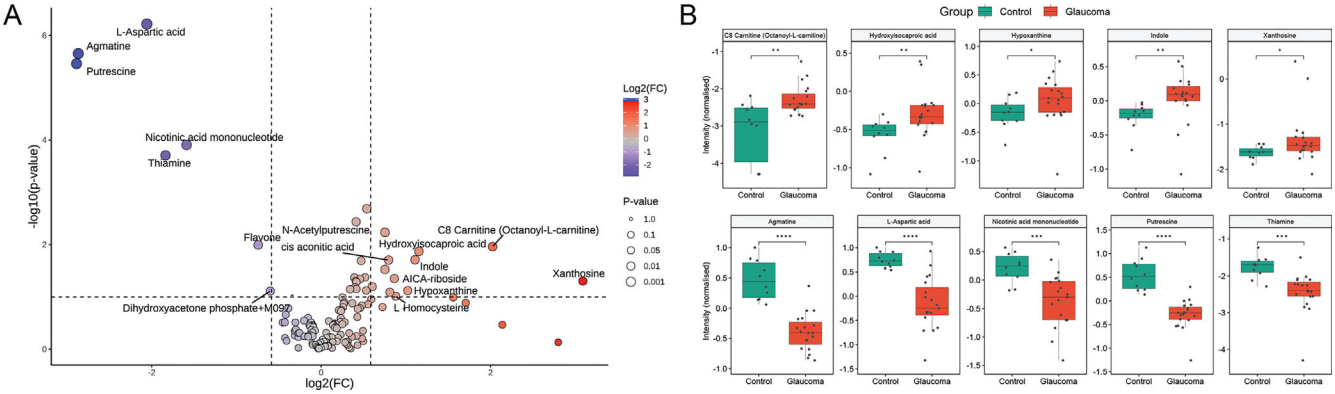

Figure 3. Glaucoma-induced dysregulation of amino acids, vitamins, and nucleic acid metabolites. (**A**) Volcano plot illustrating differentially abundant metabolites in glaucoma patients compared with healthy controls. The *x*-axis represents the $\log_2$FC, and the *y*-axis represents the $-\log_{10}(P$ value) from the Student's *t*-test. *Red circles* highlight metabolites exceeding the FC threshold of 1.5 ($\log_2$FC $\geq$ 0.5) and a *P* value threshold of 0.05 ($-\log_{10}[P$ value] $\geq$ 1.3). (**B**) Box plots showing the relative abundance of significantly altered metabolites (FC > 2; $P <$ 0.05, Student's *t*-test) in the control (*green*) and glaucoma (*red*) samples. *Boxes* represent the interquartile range, and the *line* within each box indicates the median value. *$P < 0.05$, **$P < 0.01$, ***$P < 0.001$, ****$P < 0.0001$.

tor cell line. We previously reported that these cells express TLRs and induce an inflammatory response.[28] Thus, to assess the anti-inflammatory role of these metabolites, we challenged 661W cells with TLR2 (Pam3), TLR3 (poly I:C), and TLR4 (LPS) agonists in the presence or absence of agmatine or thiamine. Our results revealed that both agmatine and thiamine treatment significantly attenuated the TLR agonist-induced inflammatory response in 661W cells (Fig. 5A). To test the neuroprotective role of agmatine and thiamine, we used an oxidative stress (H_2O_2)-induced neuronal cell death model described previously.[27] To this end, our data revealed that, compared with H_2O_2 treatment, exogenous supplementation with agmatine and thiamine protected 661W photoreceptor cells from oxidative stress–induced cell death, as revealed by a significant decrease in TUNEL-positive cells in the agmatine- or thiamine-treated groups (Fig. 5B).

Agmatine and Thiamine Treatment Alleviated the Neuroinflammatory Response and Protects RGC Function in Murine Models

After observing significant neuroprotection and anti-inflammatory responses in vitro, we evaluated the functional role of these metabolites in vivo using a mouse model of retinal neuroinflammation. TLR activation and the proinflammatory cytokine response have been shown to cause significant damage to RGCs in glaucoma.[2,34] Therefore, we induced a neuroinflammatory response in the mouse retina via intravitreal injection of TLR2 (Pam3, 0.1 µg/eye), TLR3 (poly I:C, 0.1 µg/eye), or TLR4 (LPS, 0.1 µg/eye) agonists. Six hours after TLR agonist injection, these mice were treated with either agmatine or thiamine via a single intravitreal injection. Forty-eight hours post-treatment, we performed pERG to evaluate RGC function. Our results revealed that TLR

Investigative Ophthalmology & Visual Science

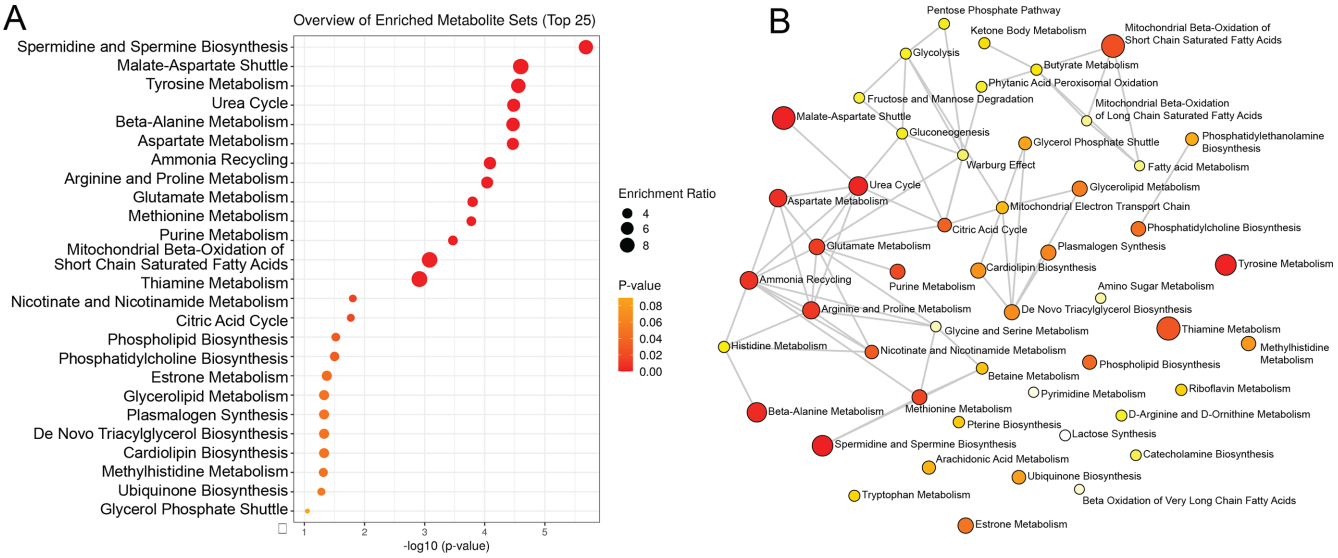

Figure 4. Dysregulated metabolites in glaucoma impact diverse essential metabolic pathways. (**A**) MSEA effectively illustrates the modulation of multiple pathways influenced by these DEMs, indicating the broad-reaching consequences of metabolite dysregulation in glaucoma. The *size* of the nodes represents the degree of influence on the relevant pathway, whereas the node *color* corresponds to the *P* value derived from a pathway enrichment analysis. (**B**) Interaction network of the pathways identified via MSEA analysis.

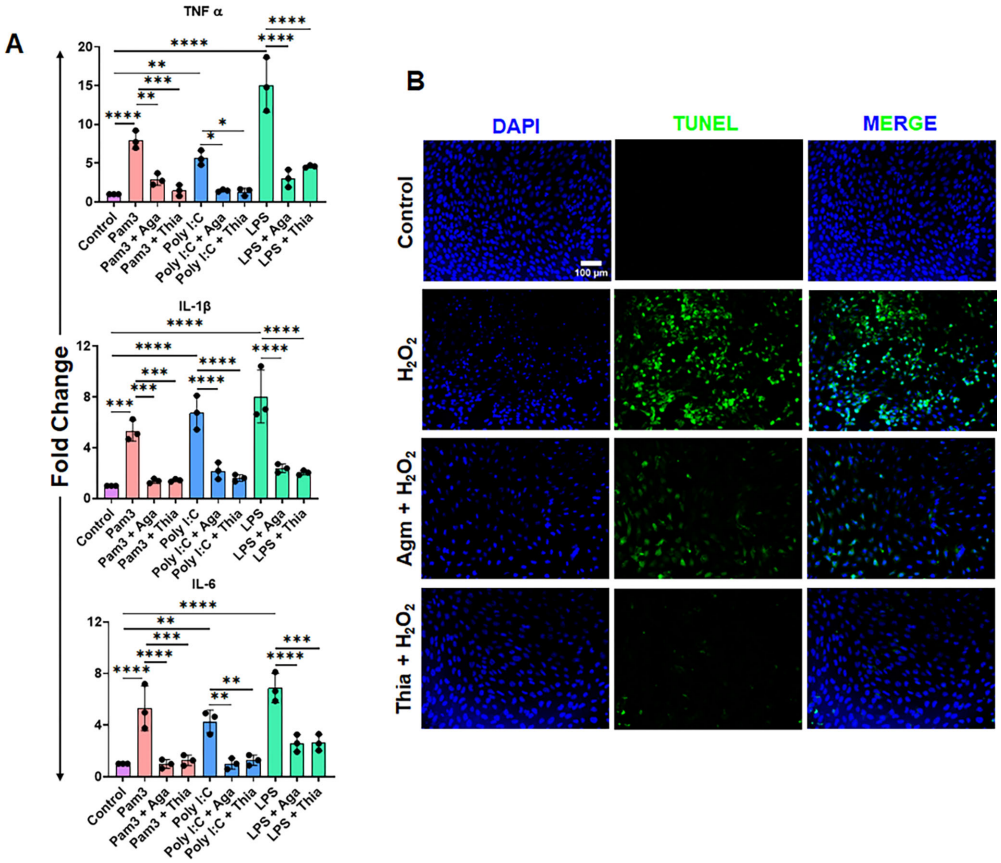

Figure 5. Agmatine and thiamine treatment attenuates the TLR-induced neuroinflammatory response and protects neuronal cells from oxidative stress-induced cell death. (**A**) Mouse cone photoreceptor cells (661W) were challenged with the TLR agonists Pam3 (TLR2), poly I:C (TLR3), and LPS (TLR4) (100 ng/mL) in the presence or absence of agmatine or thiamine (100 ng/mL) for 24 hours. The cells were harvested and subjected to qPCR to measure the transcript levels of the inflammatory cytokines TNF-α, IL-1β, and IL-6. (**B**) To assess the neuroprotective effects of agmatine and thiamine, 661W cells were challenged with H_2O_2 (100 µM) in the presence or absence of agmatine or thiamine (100 ng/mL) for 24 hours. The cells were fixed and subjected to TUNEL staining (*green*, TUNEL-positive cells; *blue*, DAPI nuclear stain). *$P < 0.05$, **$P < 0.005$, ***$P < 0.0005$, ****$P < 0.0001$ (one-way ANOVA).

Investigative Ophthalmology & Visual Science

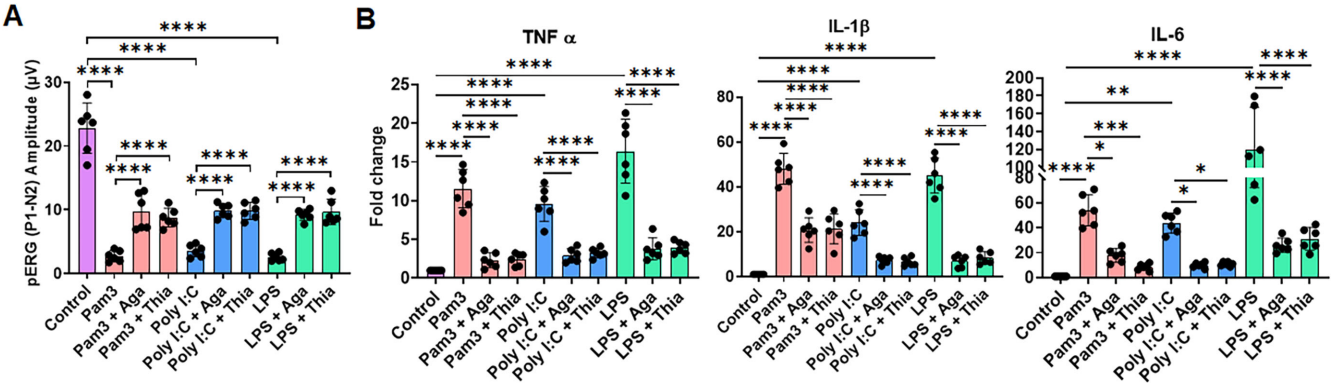

Figure 6. Agmatine and thiamine provide neuroprotection in a murine model of retinal neuroinflammation. C57BL/6 WT mice ($n = 6$) were intravitreally injected with Pam 3, poly I:C, or LPS (0.1 μg/eye) to induce retinal inflammation. After 6 hours, the eyes were treated with either agmatine or thiamine via intravitreal injection. (**A**) RGC function was assessed via pERG. The bar graph represents the pERG (P1–N2) amplitude of treated and untreated mice. (**B**) The neural retina was harvested and subjected to qPCR to measure the transcript levels of the inflammatory cytokines TNF-α, IL-1β, and IL-6. *$P < 0.05$, **$P < 0.005$, ***$P < 0.0005$, ****$P < 0.0001$ (one-way ANOVA).

agonist challenge significantly diminished RGC function, as evidenced by significant decreases in pERG wave amplitudes (Fig. 6A). However, agmatine and thiamine treatment significantly rescued pERG wave amplitudes compared with those in the untreated groups (Fig. 6A), indicating a neuroprotective role. To assess the effects of these metabolites on the inflammatory response, we harvested retinal tissue from the treated and untreated groups and performed qPCR analysis of inflammatory mediators. Our results revealed that agmatine and thiamine treatment significantly attenuated the TLR agonist-induced proinflammatory cytokine (TNFα, IL-1β, and IL-6) responses compared with that in the untreated groups (Fig. 6B).

EV-Mediated Delivery of Agmatine Via Topical Routes Attenuated the Neuroinflammatory Response of the Retina

Although intravitreal injections are commonly used to treat retinal diseases, such as diabetic retinopathy and age-related macular degeneration, noninvasive procedures are preferred by patients. Moreover, repeated intravitreal injections may lead to intraocular infections, such as endophthalmitis[35]; therefore, multiple intraocular drug delivery platforms have been optimized.[36] EV-mediated drug delivery has gained attention in recent years and has been shown to be effective in intraocular drug delivery.[37] In this study, we reasoned that EV-mediated delivery could be a noninvasive approach to deliver some of these metabolites, which can provide neuroprotection. In a proof-of-concept study, we used agmatine-loaded EVs and tested their anti-neuroinflammatory role in a mouse model of retinal neuroinflammation. First, we isolated and purified EVs from primary HTMCs. Following purification, we loaded agmatine on EVs and rigorously characterized the EV–agmatine complex for its physicochemical properties to ensure structural and physiological integrity and the loading efficiency of agmatine. Our HTMC-purified EVs met all the criteria for EVs in terms of shape and size (Fig. 7A) as per the minimal information for studies of extracellular vesicles (MISEV2023) recommendation.[32] The mean size of the HTMC-purified EVs was 146.8 ± 2.2 nm, with a concentration of 3.32×10^8 particles/mL. Our immunoblot analysis revealed that HTMC-derived EVs expressed the EV marker CD63 (Fig. 7C). We optimized the loading of agmatine in HTMC-purified EVs via previously described methods.[33] Our data show that the heat shock method can load up to 33.5 μg agmatine/mL of EVs in comparison to RT incubation, which results in 22.2 μg agmatine/mL loading (Fig. 7D). After the characterization of the EVs, we used these agmatine-loaded EVs to test their anti-neuroinflammatory potential in mice via the topical route. We induced retinal inflammation via intravitreal injection of the TLR4 agonist LPS, followed by treatment with the EV–agmatine complex once a day via eye drops (0.1 μg/eye drop). In another group of animals, an equivalent dose of agmatine (0.1 μg/eye) was injected intravitreally to compare the effects of both delivery routes. Forty-eight hours post-treatment, we harvested the neural retina and assessed the levels of pro-inflammatory cytokines via qPCR. Our results showed that EV-mediated topical delivery of agmatine significantly attenuated the LPS-induced inflammatory response in the retina compared with that in the untreated groups (Fig. 7C). Moreover, the anti-inflammatory effect of EV-mediated agmatine (topical) was comparable to that of intravitreally injected agmatine, indicating that EV-mediated topical delivery could be a potential method for treating glaucoma.

Discussion

Glaucoma is the leading cause of irreversible blindness, and current treatments are inadequate to prevent RGC damage. Therefore, the discovery of alternative neuroprotective therapies is essential for preventing or treating RGC loss in glaucoma. In the past two decades, several risk factors have been identified for glaucoma, among which metabolic dysregulation is a known risk factor. Multiple studies have indicated metabolic dysregulation in glaucoma patients; however, the comprehensive metabolic profiles of glaucoma patients are still not entirely known. The analysis of metabolomic alterations in glaucoma patients could reveal essential information regarding glaucoma pathophysiology and could also serve as a molecular biomarker for early detection and a therapeutic target for the treatment of this disease. In this pilot study, we aimed to perform targeted metabolic profiling of glaucomatous aqueous humor and test the therapeutic potential of a few key dysregulated metabolites. We accurately

Investigative Ophthalmology & Visual Science

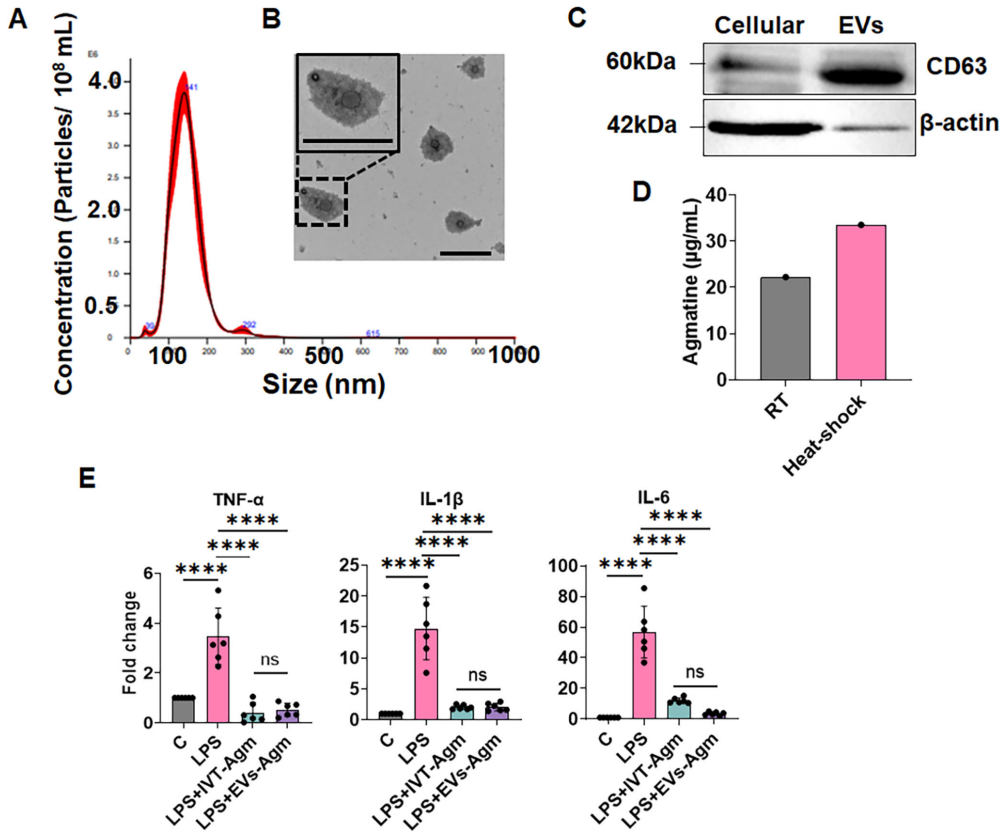

Figure 7. EV-mediated topical delivery of agmatine mitigates retinal neuroinflammation. (**A–C**) EVs were purified from HTMCs. EV size (**A**), shape (*scale bar* = 100 nm) (**B**), and enrichment for EV markers ($CD63^+$) (**C**) were assessed via NanoTracker, transmission electron microscopy, and immunoblotting analysis, respectively. (**D**) Agmatine loading was optimized using room temperature or heat shock incubation methods. (**E**) C57BL/6 mice were intravitreally injected with LPS to induce retinal inflammation. Six hours after LPS injection, agmatine-loaded EVs were applied as eye drops once a day. In another group of mice, 6 hours after LPS injection agmatine was injected intravitreally. After 48 hours of agmatine treatment, the mouse neural retina was harvested and subjected to qPCR to measure the transcript levels of the inflammatory cytokines TNF-α, IL-1β, and IL-6. *$P < 0.05$, **$P < 0.005$, ***$P < 0.0005$, and ****$P < 0.0001$ (one-way ANOVA).

measured ~135 endogenous metabolites, among which ~31 DEMs were significantly dysregulated in glaucomatous aqueous humor compared with healthy controls. Many of these altered metabolites belong to the carbohydrate (dihydroxyacetone phosphate), lipid (dihydroxyacetone phosphate, choline), DNA (xanthosine, hypoxanthine, thymidine), amino acid (aspartic acid, proline), vitamin (thiamine, nicotinic acid mononucleotide), and polyamine (carnitine, putrescine, agmatine) families. Among the DEMs, carnitine (octanoyl-L-carnitine), hydroxyisocaproic acid, indole, xanthosine, and hypoxanthine were significantly elevated in the aqueous humor of POAG patients. In contrast, L-aspartic acid, agmatine, putrescine, nicotinic acid mononucleotide, and thiamine levels were significantly decreased in the aqueous humor of POAG patients. These altered metabolites regulate multiple key cellular metabolic processes, including energy metabolism and fatty acid synthesis, indicating the disruption of critical cellular functions during glaucoma. Our findings are in line with those of previous studies showing metabolic changes in glaucoma patients; however, each of these studies is unique in identifying completely unique sets of metabolites. For example, Myer et al.[6] reported alterations in several amino acids, such as arginine, lysine, cysteine, and glycine (increased), as well as phenylalanine, threonine, and glutamine (decreased), in addition to anthranilate, ascorbate, myo-inositol, acetate, 2-hydroxy butyrate, creatine, and choline in the aqueous humor from POAG patients. Buisset et al.[21] identified reduced concentrations of taurine and spermine and increased concentrations of creatinine, carnitine, acylcarnitines, and several amino acids, such as glutamine, glycine, alanine, and leucine, in the aqueous humor of POAG patients compared with those of healthy patients. Another study by Botello-Marabotto and coworkers[38] reported an increase in the concentrations of glycine, urea, and glucose and a decrease in the concentrations of phenylalanine, phenylacetate, leucine, and formic acid in tears from POAG patients. Barbosa Breda et al.[18] reported increased concentrations of *N*-acetylglutamate and glutamate, suggesting that these changes are associated with excitotoxicity in glaucoma. Many of these altered metabolites are known to modulate key biological processes that have been implicated in the regulation of aqueous humor production and outflow pathways. Moreover, some of these altered metabolites, such as taurine and creatine, have been reported to have immunomodulatory and neuroprotective effects against neuroinflammation and oxidative and osmotic stress.[17,38] In glaucoma patients, we observed increases in octanoyl-L-carnitine, which is a derivative of L-carnitine that could offer antioxidant, anti-apoptotic, and osmoregulatory benefits in glaucoma. Similarly, indole, particularly indole-3-acetic acid, has been shown to suppress glaucoma and

myopia progression by promoting type I collagen synthesis. Agmatine has a hypotensive effect in glaucoma. Further investigation of the neuroprotective potential of these metabolites in glaucomatous neurodegeneration might be needed.

In the present study, we identified significantly decreased levels of a polyamine family metabolite and a putative neuromodulator (agmatine) and vitamin B1 (thiamine) in glaucomatous aqueous humor which has not been reported previously in any of the glaucoma metabolomics studies. Agmatine has been shown to interact with *N*-methyl-D-aspartate (NMDA) and α2-adrenoceptors, indicating its role in enhancing cell viability, neuronal protection, and synaptic plasticity.[39] Similarly, vitamin B1 deficiency has been linked to glaucoma[40] and degeneration of ganglion cells in the brain and spinal cord in animal models.[41] These studies are in consonance with our observations of reduced concentrations of agmatine and thiamine in glaucoma patients, implicating their role in the pathophysiology of this disease. Therefore, in the present study, we aimed to test the anti-neuroinflammatory and neuroprotective abilities of these two metabolites, agmatine and thiamine, using in vitro and in vivo models of retinal neuroinflammation. To test the anti-neuroinflammatory properties of these metabolites in vitro, we challenged mouse neuronal cone photoreceptor cells with various TLR agonists (TLR2, TLR3, and TLR4) in the presence or absence of agmatine or thiamine and measured the transcript levels of pro-inflammatory cytokines. Our data showed that agmatine and thiamine treatment significantly reduced the TLR-induced inflammatory response. Moreover, agmatine and thiamine treatment also rescued photoreceptor cells from oxidative stress–induced cell death, confirming their neuroprotective abilities. Our findings corroborated those of a previous study showing the anti-inflammatory role of agmatine in LPS-activated BV2 microglia.[42] To further confirm the anti-neuroinflammatory and neuroprotective effects of these metabolites in vivo, we intravitreally injected agmatine or thiamine in a mouse model of retinal neuroinflammation. Our results showed that a single intravitreal injection of agmatine or thiamine attenuated TLR-induced retinal inflammation. Moreover, agmatine and thiamine treatment reversed the pERG wave response in inflammation-induced RGC damage, indicating its neuroprotective potential. To further optimize the intraocular delivery of metabolites via the topical route, we loaded agmatine in EVs, which significantly attenuated LPS-induced intraocular inflammation. These findings confirm that the intravitreal and topical delivery of agmatine or thiamine can provide neuroprotection in murine models of retinal neuroinflammation. Although we observed comparable protective effects via intravitreal and EV-mediated topical delivery, additional studies are needed to investigate whether the topical application of EVs loaded with neuroprotective metabolites can reduce the dosage and frequency of intraocular applications. Our findings support the previous findings, where agmatine has been demonstrated to reduce the proinflammatory response in brain injury[43] and retinal damage in ischemic injury,[44] lower IOP, and protect RGCs in an ocular hypertensive rat model.[45] Similarly, thiamine has been shown to play a neuroprotective role in memory impairment and the suppression of proinflammatory cytokines in traumatic brain injury.[46] Although these metabolites have shown protection in different disease models, their neuroprotective abilities in glaucoma and their efficacy via different delivery routes must be evaluated.

We demonstrated metabolic alterations in the aqueous humor of POAG patients, but our study has several limitations. This pilot study employed a relatively small sample size (29 patients: 19 POAG and 10 normal subjects), which may affect the accurate assessment of the metabolomic profiles in the glaucoma population. Our future studies will focus on a larger cohort of glaucoma patients and use a paired matrix (plasma and aqueous humor from the same patient) to identify the global metabolomic profiles of ocular and systemic circulation. Metabolomics studies from paired matrices from the same subjects could help us determine potential biomarkers for early diagnosis or therapeutics for glaucoma. As mentioned by Myer et al.,[6] glaucoma patients are taking IOP-lowering medications; therefore, it is uncertain whether the metabolic alteration in glaucoma patients is due to the disease itself or the effect of medication, which could be another limitation of such studies. Moreover, other factors, such as disease severity, diurnal fluctuations in IOP, aqueous humor outflow, and time of collection, can also contribute to the alterations in metabolite compositions.[6] Although these limitations are inherent to any such human studies, we still observed marked differences in the metabolomic profiles of glaucoma patients and healthy subjects.

In conclusion, our study revealed metabolomic alterations in the aqueous humor of POAG patients and identified dysregulation of 31 DEMs that modulate multiple key cellular metabolic pathways. Among these DEMs, agmatine and thiamine have shown anti-neuroinflammatory and neuroprotective potential in mouse models of retinal neuroinflammation. Our future studies will focus on creating RGC-specific EVs by labeling them with RGC-specific antibodies and testing the anti-neuroinflammatory and neuroprotective properties of agmatine and thiamine in glaucoma.

Acknowledgments

The authors thank Muayyad Al-Ubaidi, PhD (Department of Cell Biology, University of Oklahoma Health Sciences Center, Oklahoma City, OK) for sharing the 661W cell line.

Supported in part by the National Institutes of Health (NIH) Clinical and Translational Science Award UL1TR002345; the NIH/National Eye Institute grant R01EY032495; University of Missouri School of Medicine start-up funds to PKS; the Kresge Eye Institute Translational Research Investigation Award (KEI-TRIG) to PKS and AK; and NIH grants R01EY035499, R01EY026964, and R01EY027381 to AK. The funders had no role in the study design, data collection, interpretation, or decision to submit this work for publication.

Author Contributions: M.M. performed the experiments, analyzed the data, and prepared the manuscript draft. B.K. performed the metabolomics data analysis. R.A. and A.S. assisted with purification, characterization, and drug loading on EVs. N.N., V.P., S.D., S. S., M.K., B.A.H., and M.S.J. helped with aqueous humor collection from the OR. V.R. assisted with the demographic and clinical history of the patients. A.K. conceived the idea, provided resources and funding, and edited the manuscript. P.K.S. conceived the idea, designed and supervised the study, provided funding/regents/analysis tools, analyzed the data, and wrote the manuscript. All the authors read and approved the final version of the manuscript.

Disclosure: **M. Monu**, None; **B. Kumar**, None; **R. Asfiya**, None; **N. Nassiri**, None; **V. Patel**, None; **S. Das**, None; **S. Syeda**, None; **M. Kanwar**, None; **V. Rajeswaren**, None; **B.A. Hughes**, None;

M.S. Juzych, None; **A. Srivastava**, None; **A. Kumar**, None; **P.K. Singh**, None

References

1. Hwang S, Choi S, Choi SH, Kim KY, Miller YI, Ju WK. Apolipoprotein A-I binding protein-mediated neuroprotection in glaucomatous neuroinflammation and neurodegeneration. *Neural Regen Res*. 2025;20:1414–1415.
2. Tezel G. Molecular regulation of neuroinflammation in glaucoma: current knowledge and the ongoing search for new treatment targets. *Prog Retin Eye Res*. 2022;87:100998.
3. Jayaram H, Kolko M, Friedman DS, Gazzard G. Glaucoma: now and beyond. *Lancet*. 2023;402:1788–1801.
4. Rolle T, Ponzetto A, Malinverni L. The role of neuroinflammation in glaucoma: an update on molecular mechanisms and new therapeutic options. *Front Neurol*. 2020;11:612422.
5. Kasetti RB, Patel PD, Maddineni P, et al. ATF4 leads to glaucoma by promoting protein synthesis and ER client protein load. *Nat Commun*. 2020;11:5594.
6. Myer C, Perez J, Abdelrahman L, et al. Differentiation of soluble aqueous humor metabolites in primary open angle glaucoma and controls. *Exp Eye Res*. 2020;194:108024.
7. Rossi C, Cicalini I, Cufaro MC, et al. Multi-omics approach for studying tears in treatment-naive glaucoma patients. *Int J Mol Sci*. 2019;20:4029.
8. Li X, Cai S, He Z, et al. Metabolomics in retinal diseases: an update. *Biology (Basel)*. 2021;10:944.
9. Liu H, Prokosch V. Energy metabolism in the inner retina in health and glaucoma. *Int J Mol Sci*. 2021;22:3689.
10. Zhu J, Thompson CB. Metabolic regulation of cell growth and proliferation. *Nat Rev Mol Cell Biol*. 2019;20:436–450.
11. Zhang Q, Wang N, Rui Y, Xia Y, Xiong S, Xia X. New insight of metabolomics in ocular diseases in the context of 3P medicine. *EPMA J*. 2023;14:53–71.
12. Takata N, Miska JM, Morgan MA, et al. Lactate-dependent transcriptional regulation controls mammalian eye morphogenesis. *Nat Commun*. 2023;14:4129.
13. Viegas FO, Neuhauss SCF. A metabolic landscape for maintaining retina integrity and function. *Front Mol Neurosci*. 2021;14:656000.
14. Shu DY, Chaudhary S, Cho KS, et al. Role of oxidative stress in ocular diseases: a balancing act. *Metabolites*. 2023;13:187.
15. Kominsky DJ, Campbell EL, Colgan SP. Metabolic shifts in immunity and inflammation. *J Immunol*. 2010;184:4062–4068.
16. Hanna J, David LA, Touahri Y, Fleming T, Screaton RA, Schuurmans C. Beyond genetics: the role of metabolism in photoreceptor survival, development and repair. *Front Cell Dev Biol*. 2022;10:887764.
17. Tang Y, Shah S, Cho KS, Sun X, Chen DF. Metabolomics in primary open angle glaucoma: a systematic review and meta-analysis. *Front Neurosci*. 2022;16:835736.
18. Barbosa Breda J, Croitor Sava A, Himmelreich U, et al. Metabolomic profiling of aqueous humor from glaucoma patients - the metabolomics in surgical ophthalmological patients (MISO) study. *Exp Eye Res*. 2020;201:108268.
19. Mayordomo-Febrer A, López-Murcia M, Morales-Tatay JM, Monleón-Salvado D, Pinazo-Durán MD. Metabolomics of the aqueous humor in the rat glaucoma model induced by a series of intracamerular sodium hyaluronate injection. *Exp Eye Res*. 2015;131:84–92.
20. Tang Y, Pan Y, Chen Y, et al. Metabolomic profiling of aqueous humor and plasma in primary open angle glaucoma patients points towards novel diagnostic and therapeutic strategy. *Front Pharmacol*. 2021;12:621146.
21. Buisset A, Gohier P, Leruez S, et al. Metabolomic profiling of aqueous humor in glaucoma points to taurine and spermine deficiency: findings from the Eye-D study. *J Proteome Res*. 2019;18:1307–1315.
22. Zeleznik OA, Kang JH, Lasky-Su J, et al. Plasma metabolite profile for primary open-angle glaucoma in three US cohorts and the UK Biobank. *Nat Commun*. 2023;14:2860.
23. Gowtham L, Halder N, Angmo D, et al. Untargeted metabolomics in the aqueous humor reveals the involvement of TAAR pathway in glaucoma. *Exp Eye Res*. 2023;234:109592.
24. Leruez S, Marill A, Bresson T, et al. A metabolomics profiling of glaucoma points to mitochondrial dysfunction, senescence, and polyamines deficiency. *Invest Ophthalmol Vis Sci*. 2018;59:4355–4361.
25. Yue Y, Bao X, Jiang J, Li J. Evaluation and correction of injection order effects in LC-MS/MS based targeted metabolomics. *J Chromatogr B Analyt Technol Biomed Life Sci*. 2022;1212:123513.
26. Kuhl C, Tautenhahn R, Bottcher C, Larson TR, Neumann S. CAMERA: an integrated strategy for compound spectra extraction and annotation of liquid chromatography/mass spectrometry data sets. *Anal Chem*. 2012;84:283–289.
27. Boss JD, Singh PK, Pandya HK, et al. Assessment of neurotrophins and inflammatory mediators in vitreous of patients with diabetic retinopathy. *Invest Ophthalmol Vis Sci*. 2017;58:5594–5603.
28. Singh PK, Kumar A. Retinal photoreceptor expresses toll-like receptors (TLRs) and elicits innate responses following TLR ligand and bacterial challenge. *PLoS One*. 2015;10:e0119541.
29. Tan E, Ding XQ, Saadi A, Agarwal N, Naash MI, Al-Ubaidi MR. Expression of cone-photoreceptor-specific antigens in a cell line derived from retinal tumors in transgenic mice. *Invest Ophthalmol Vis Sci*. 2004;45:764–768.
30. Srivastava A, Amreddy N, Babu A, et al. Nanosomes carrying doxorubicin exhibit potent anticancer activity against human lung cancer cells. *Sci Rep*. 2016;6:38541.
31. Théry C, Amigorena S, Raposo G, Clayton A. Isolation and characterization of exosomes from cell culture supernatants and biological fluids. *Curr Protoc Cell Biol*. 2006;Chapter 3:Unit 3.22.
32. Welsh JA, Goberdhan DCI, O'Driscoll L, et al. Minimal information for studies of extracellular vesicles (MISEV2023): from basic to advanced approaches. *J Extracell Vesicles*. 2024;13:e12404.
33. Kim H, Kang JY, Mun D, Yun N, Joung B. Calcium chloride enhances the delivery of exosomes. *PLoS One*. 2019;14:e0220036.
34. Vernazza S, Oddone F, Tirendi S, Bassi AM. Risk factors for retinal ganglion cell distress in glaucoma and neuroprotective potential intervention. *Int J Mol Sci*. 2021;22:7994.
35. Sachdeva MM, Moshiri A, Leder HA, Scott AW. Endophthalmitis following intravitreal injection of anti-VEGF agents: long-term outcomes and the identification of unusual micro-organisms. *J Ophthalmic Inflamm Infect*. 2016;6:2.
36. Wykoff CC, Kuppermann BD, Regillo CD, et al. Extended intraocular drug-delivery platforms for the treatment of retinal and choroidal diseases. *J Vitreoretin Dis*. 2024;8:577–586.
37. Massoumi H, Amin S, Soleimani M, et al. Extracellular-vesicle-based therapeutics in neuro-ophthalmic disorders. *Int J Mol Sci*. 2023;24:9006.
38. Botello-Marabotto M, Martínez-Bisbal MC, Pinazo-Durán MD, Martínez-Máñez R. Tear metabolomics for the diagnosis of primary open-angle glaucoma. *Talanta*. 2024;273:125826.

39. Rafi H, Rafiq H, Farhan M. Pharmacological profile of agmatine: an in-depth overview. *Neuropeptides*. 2024;105:102429.
40. Asregadoo ER. Blood levels of thiamine and ascorbic acid in chronic open-angle glaucoma. *Ann Ophthalmol*. 1979;11:1095–1100.
41. Head KA. Natural therapies for ocular disorders, part two: cataracts and glaucoma. *Altern Med Rev*. 2001;6:141–166.
42. Milosevic K, Stevanovic I, Bozic ID, et al. Agmatine mitigates inflammation-related oxidative stress in BV-2 cells by inducing a pre-adaptive response. *Int J Mol Sci*. 2022;23:3561.
43. Feng Y, LeBlanc MH. Effect of agmatine on the time course of brain inflammatory cytokines after injury in rat pups. *Ann N Y Acad Sci*. 2003;1009:152–156.
44. Hong S, Hara H, Shimazawa M, Hyakkoku K, Kim CY, Seong GJ. Retinal protective effects of topically administered agmatine on ischemic ocular injury caused by transient occlusion of the ophthalmic artery. *Braz J Med Biol Res*. 2012;45:212–215.
45. Hong S, Kim CY, Lee WS, Shim J, Yeom HY, Seong GJ. Ocular hypotensive effects of topically administered agmatine in a chronic ocular hypertensive rat model. *Exp Eye Res*. 2010;90:97–103.
46. Husn M, Amin Z, Ali Y, et al. Neuroprotective effects of vitamin B1 on memory impairment and suppression of pro-inflammatory cytokines in traumatic brain injury. *Metab Brain Dis*. 2023;38:2175–2184.

Investigative Ophthalmology & Visual Science